Image-current detection of antiprotons

Christian Smorra (BASE collaboration)
RIKEN Fundamental Symmetries Laboratory

AVA Summer School

27. 06. 2018

Main Principle

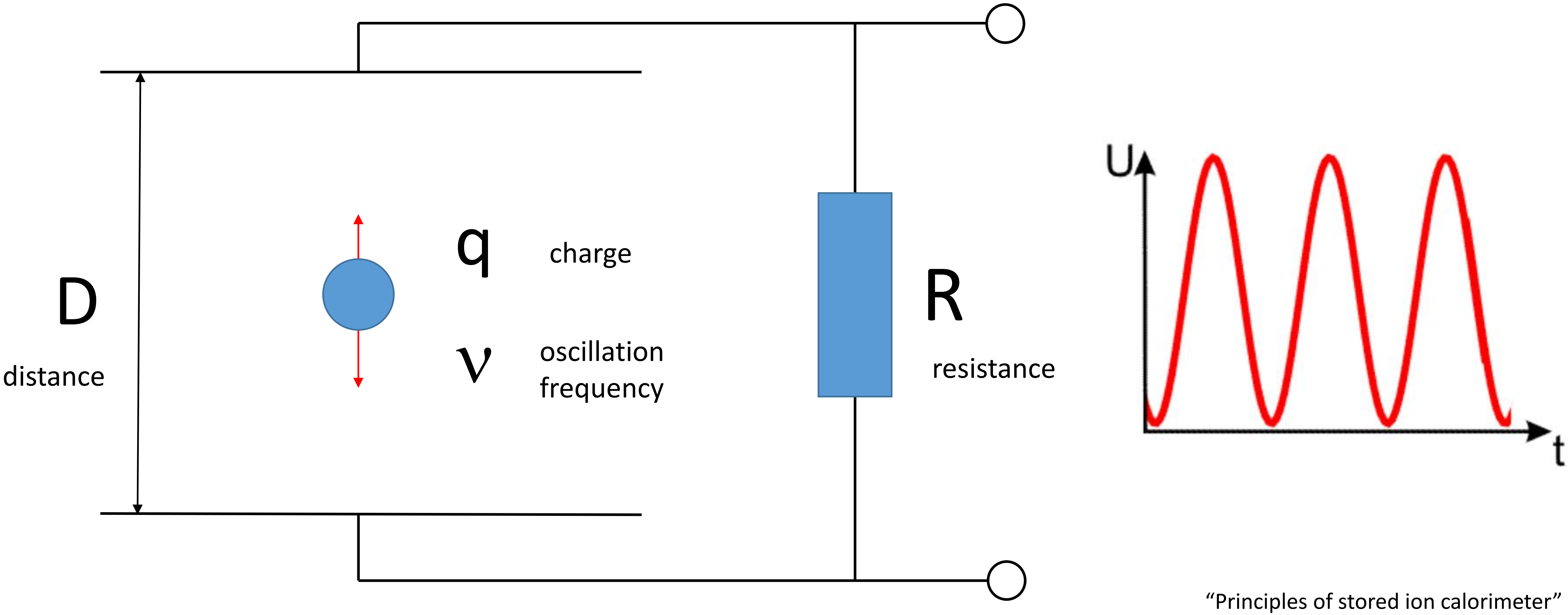

"Principles of stored ion calorimeter"
D.J. Wineland, H. G. Dehmelt,
J. Appl. Phys. **46**, 919 (1975).

Image-current detector in action

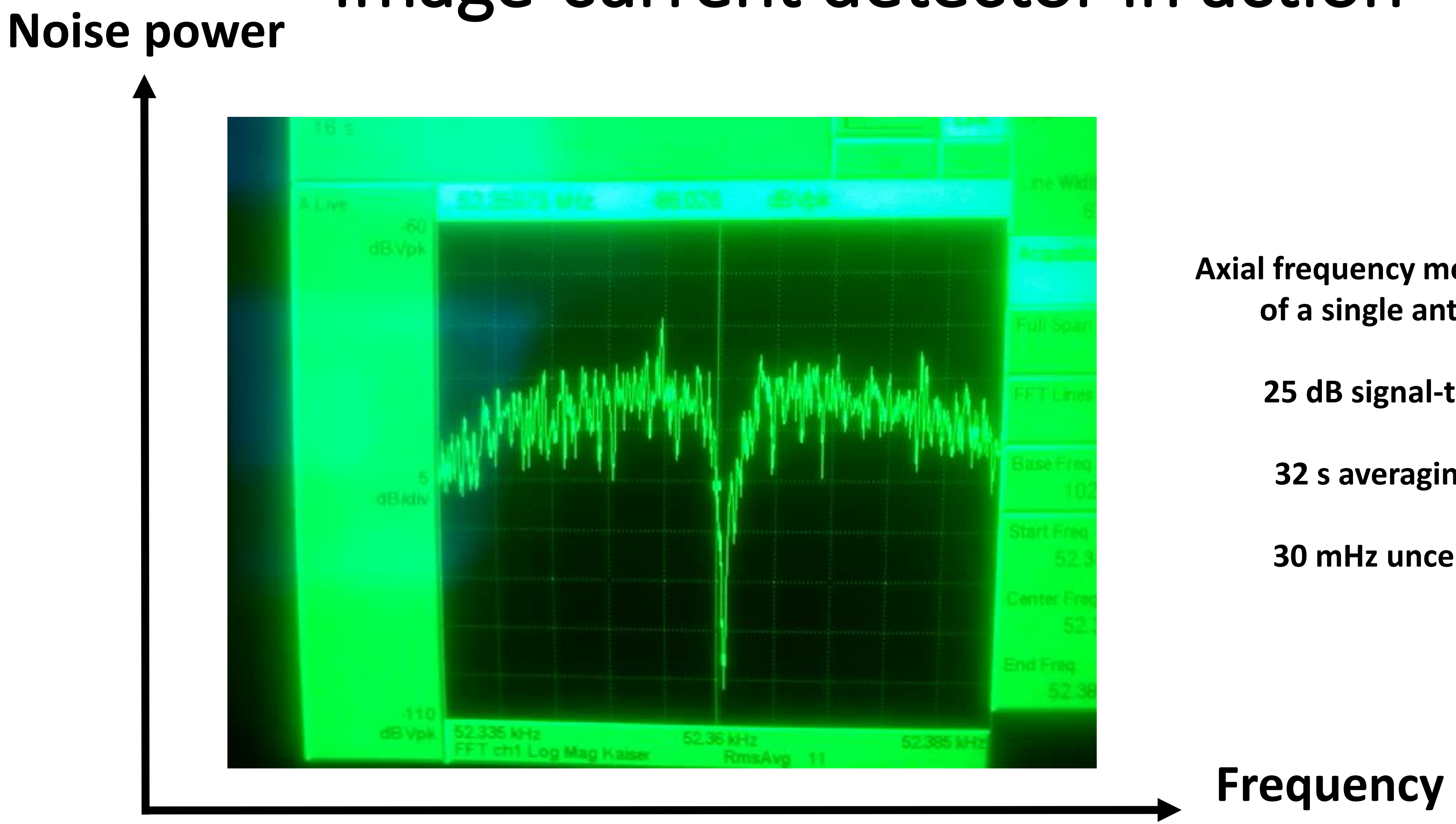

Axial frequency measurement of a single antiproton

25 dB signal-to-noise

32 s averaging time

30 mHz uncertainty

What can we do with this technique?

- Non-destructively detect antiprotons
- Resistively cool antiprotons (T < 2 K, E < 50 mK)
- Count the number of trapped antiprotons
- Observe the spin state of single antiprotons
- Measure trap oscillation frequencies with 30 mHz uncertainty

- **Highly-sensitive tests of CPT invariance in the baryon sector**
  - Antiproton charge-to-mass ratio (69 ppt)
  - Antiproton magnetic moment (1.5 ppb)
  - Antiproton lifetime in vacuum (> 10 years)
- **A lot of other physics as well (e.g. nuclear physics, neutrino physics, …)**

Content

- Motion in a Penning trap
- Image-current detection principles and methods
- Resistive cooling
- Sideband cooling
- Construction of a single particle detector
  - Axial detector (~ 680 kHz)
  - Cyclotron detector (~ 30 - 75 MHz)

Step 1: Make a single particle harmonic oscillator

A single antiproton in a Penning-trap:

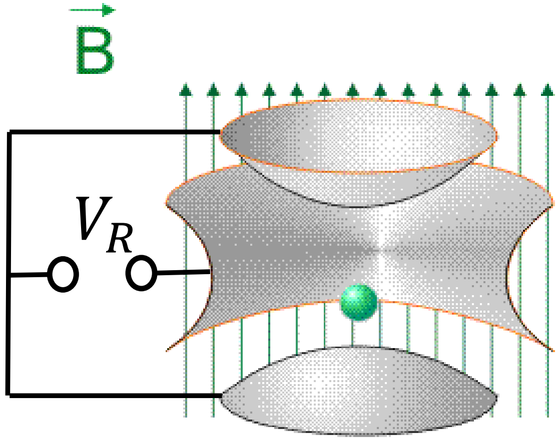

Magnetic field: $\vec{B} = B_0 \, \hat{e}_z$

Quadrupole potential: $V(\rho, z) = V_R C_2 \left(z^2 - \frac{\rho^2}{2} \right)$

We **choose** the electrode geometry and potential configuration **to a make a single particle harmonic oscillators** along the magnetic field lines!

Motion in a Penning trap

Harmonic axial motion: $\omega_z = \sqrt{\frac{2\,q\,C_2\,V_R}{m}}$

Radial plane:

- Lorentz force pointing to center
- Electrostatic force pointing outwards

Result: Two harmonic-oscillator(-like) modes:

$$\omega_\pm = \frac{\omega_c}{2} \pm \sqrt{\frac{\omega_c^2}{4} - \frac{\omega_z^2}{2}}$$

Modified cyclotron mode: Mainly kinetic energy

Magnetron mode: Metastable, mainly negative potential energy

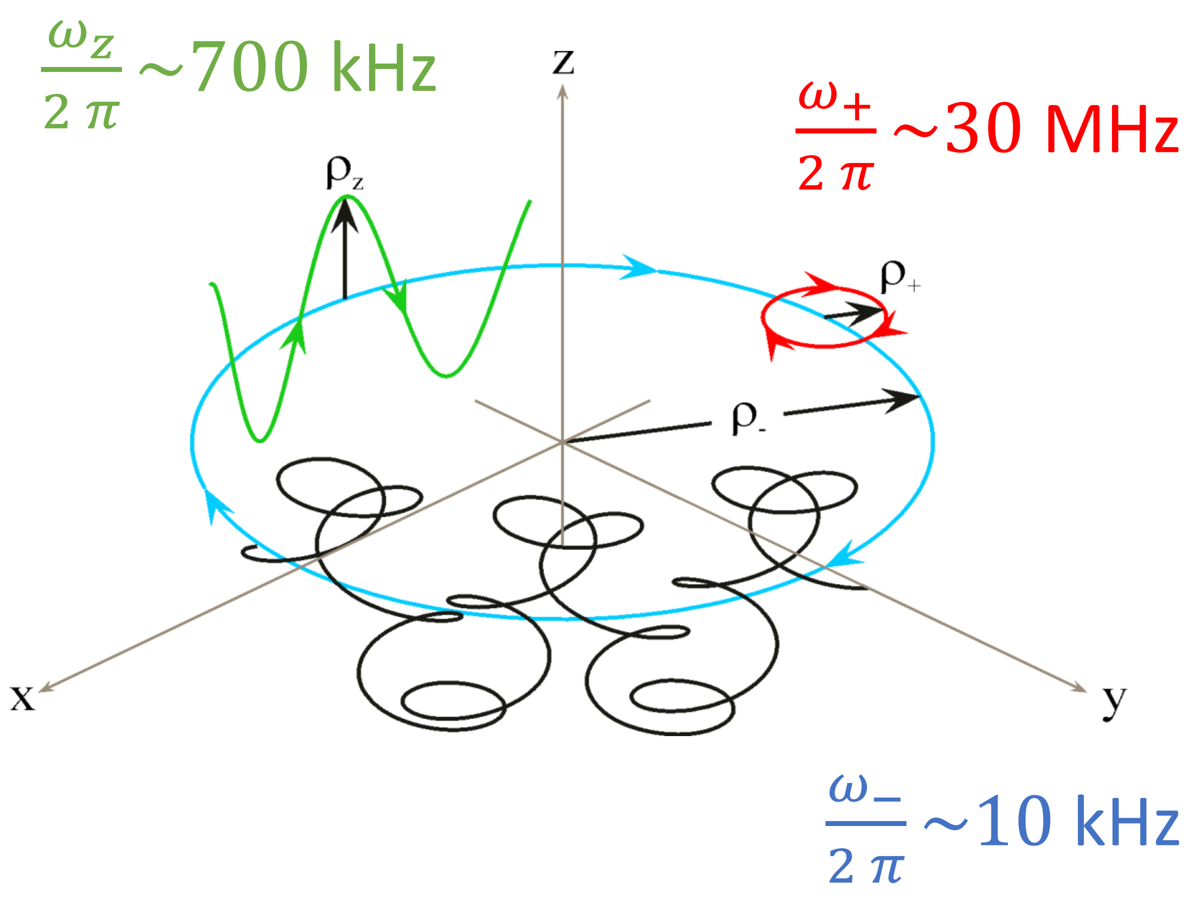

L.S. Brown and G. Gabrielse, *Rev. Mod. Phys.* **58**, 233-311, (1986)

Image-current detection methods

Image-current detection

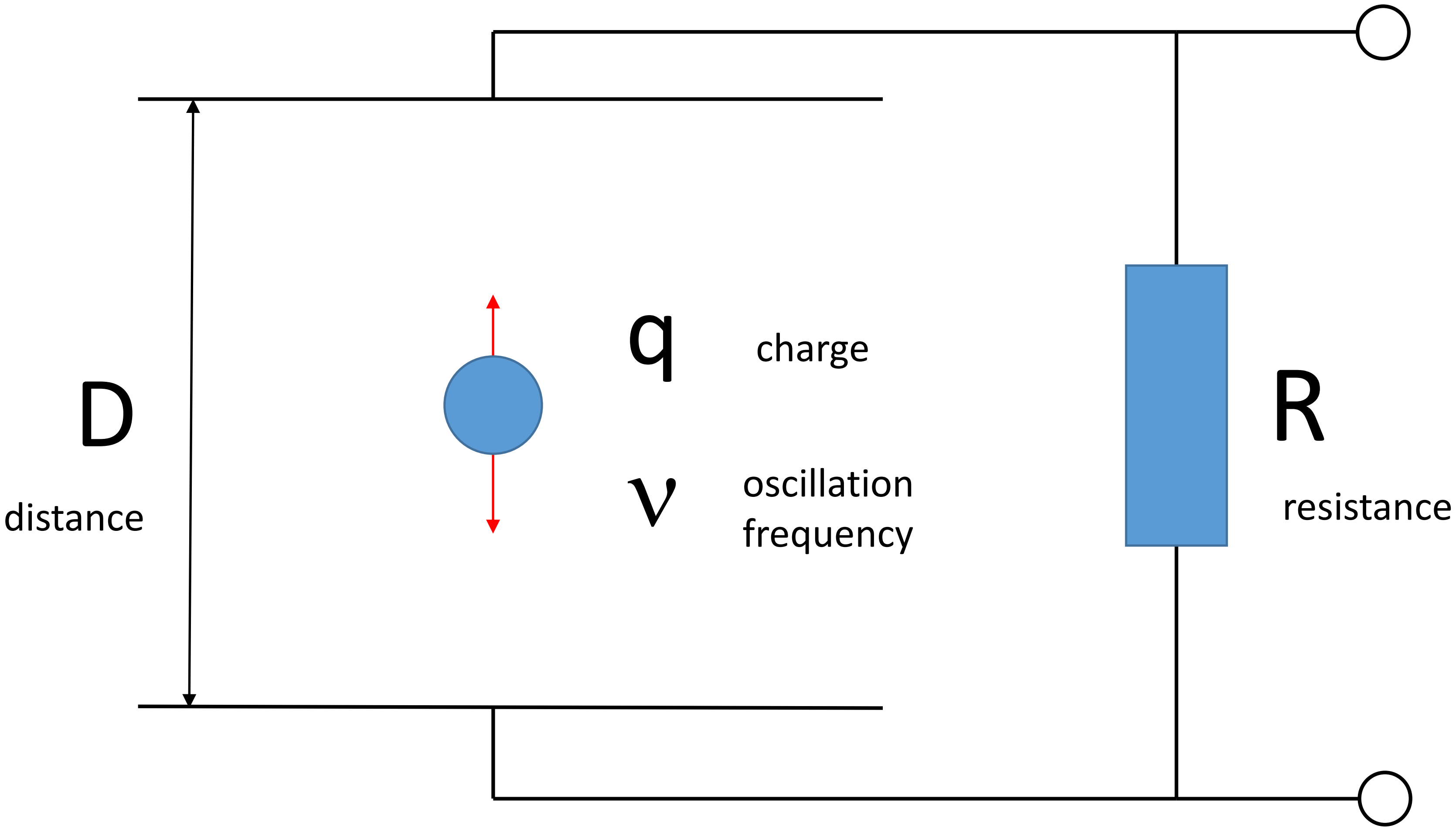

Energy balance:

$$U\ I\ \partial t = F\ v\ \partial t$$

Image current:

$$I = \frac{q}{D} 2\pi\ \nu\ z$$

Example:

Axial Mode of a single antiproton:

q = 1.6 10^{-19} C

D = 1 cm

z = 0.1 mm

ν = 1 MHz

$$I \sim 10^{-14}\ \text{A}$$

A detection circuit for fA currents

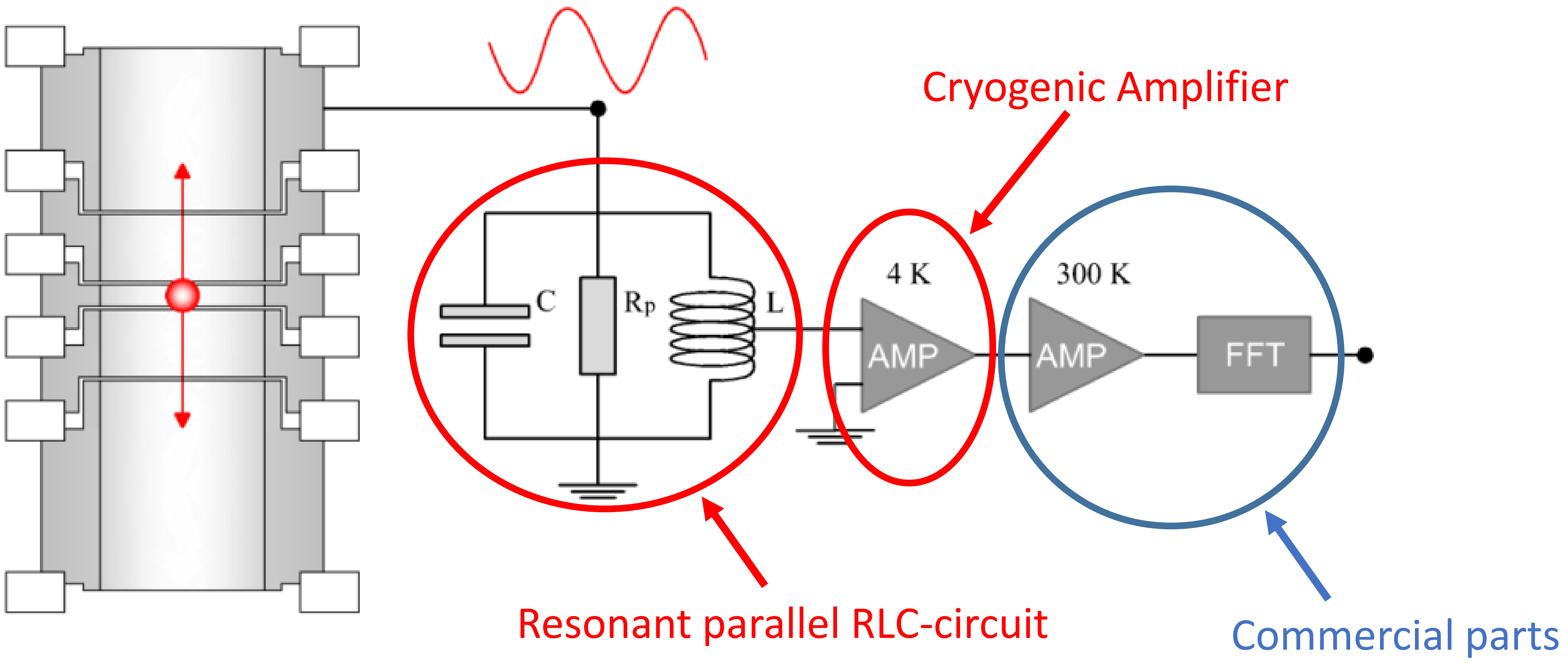

RLC-Circuit Components

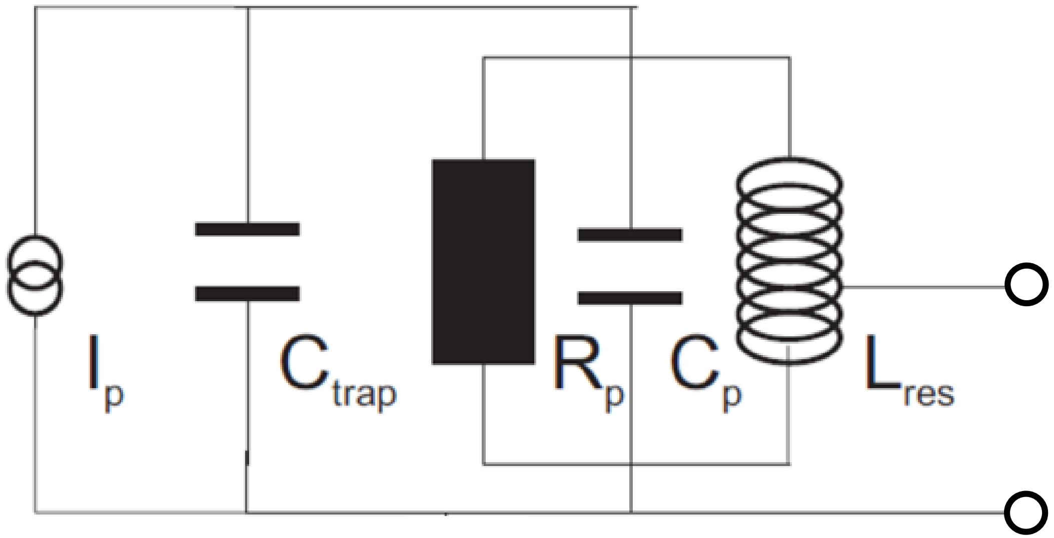

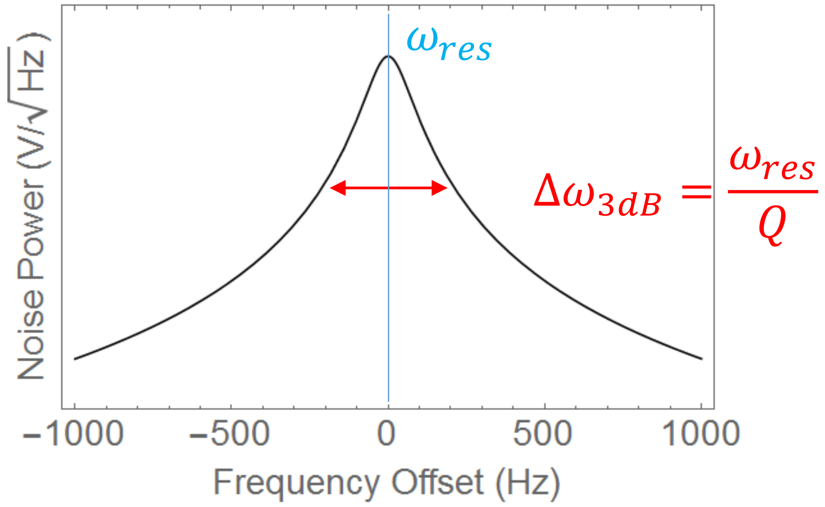

I_p **Particle:** Current source

Tuned circuit:

$$\omega_{res} = \frac{1}{\sqrt{L\,C}}$$

R_p Parallel resistance:
Damping! (a parasitic property)

$$R_s = R_p/Q^2$$

Q Energy loss per oscillation cycle

L_{res} Inductance:
Added to compensate the parasitic capacitance at the particle frequency

C_{trap} Parasitic Capacitance:
Capacitance of the detection electrode to ground

C_p Capacitance of your detection system to ground

Peak detection

- Particle dissipates power in the parallel resistance
  - Detection (FFT)
  - Cooling (time constant 2 min)

1. No signal
   Particle in thermal equilibrium
2. Excitation at the modified cyclotron frequency
3. FFT Reset
4. Peak signal at the modified cyclotron frequency

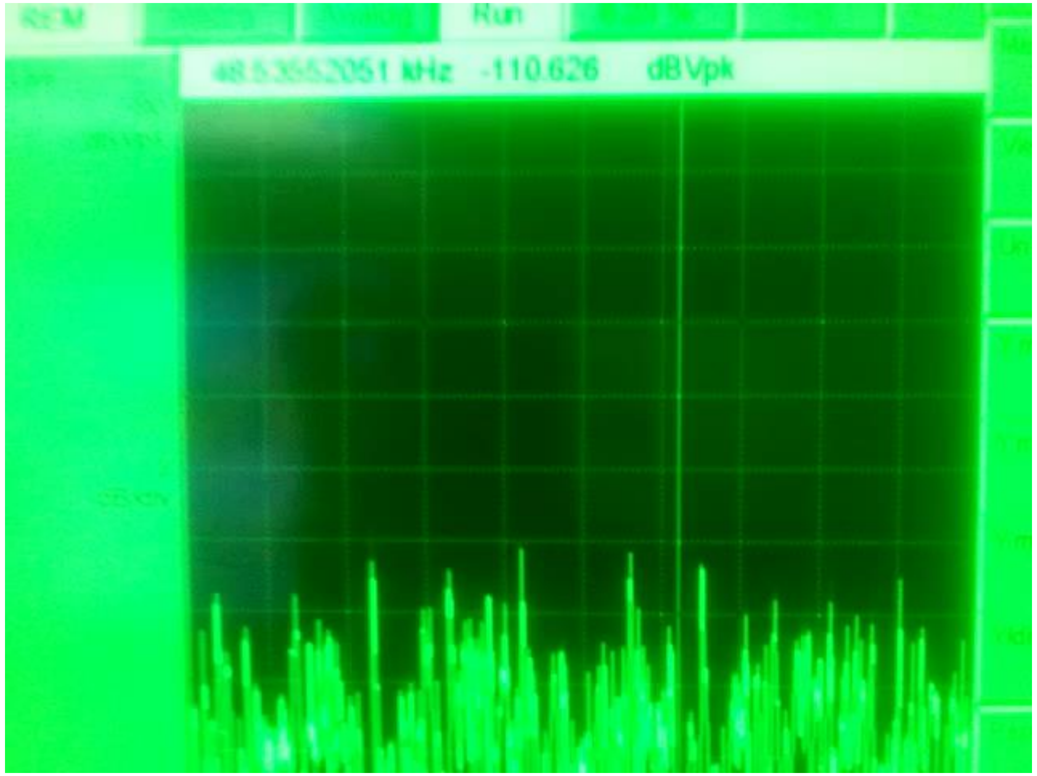

Resistive cooling

$$\tau = \frac{m}{q^2}\frac{D^2}{R_p}$$

Cyclotron mode: $\tau \sim 1$ min

Axial mode: $\tau \sim 30$ ms

Damped harmonic oscillator

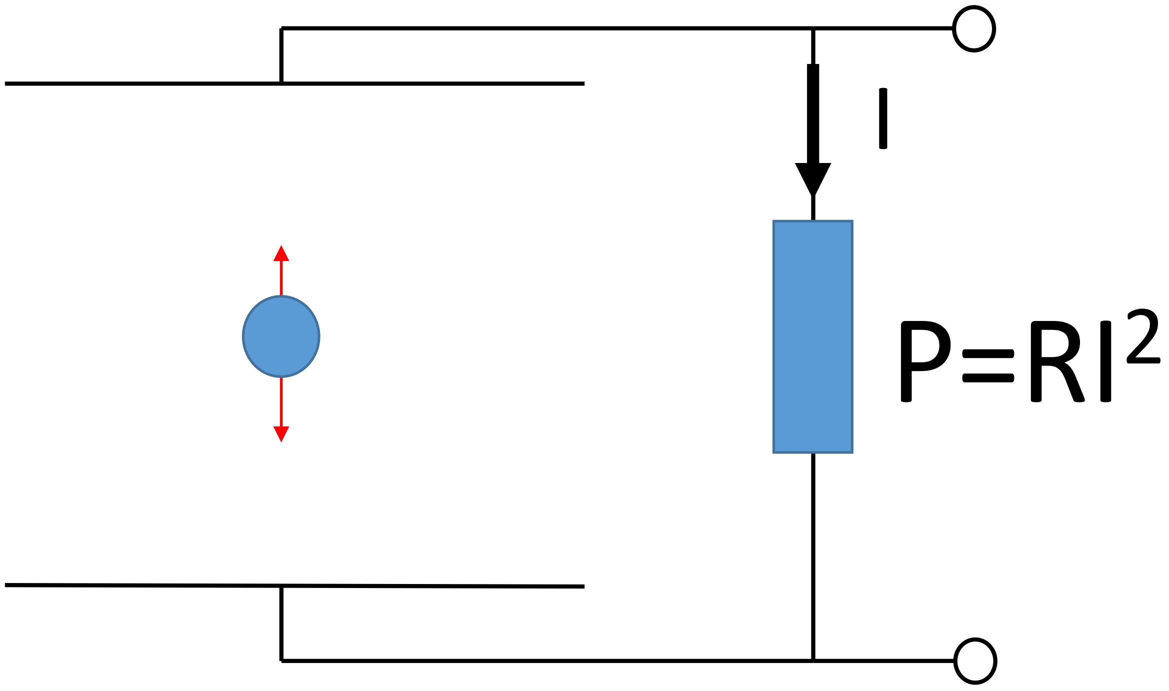

Amplitude-dependent frequency shifts:

- Relativistic shift $\propto E_+$
- Residual magnetic bottle ($\propto B_2 E_+$)

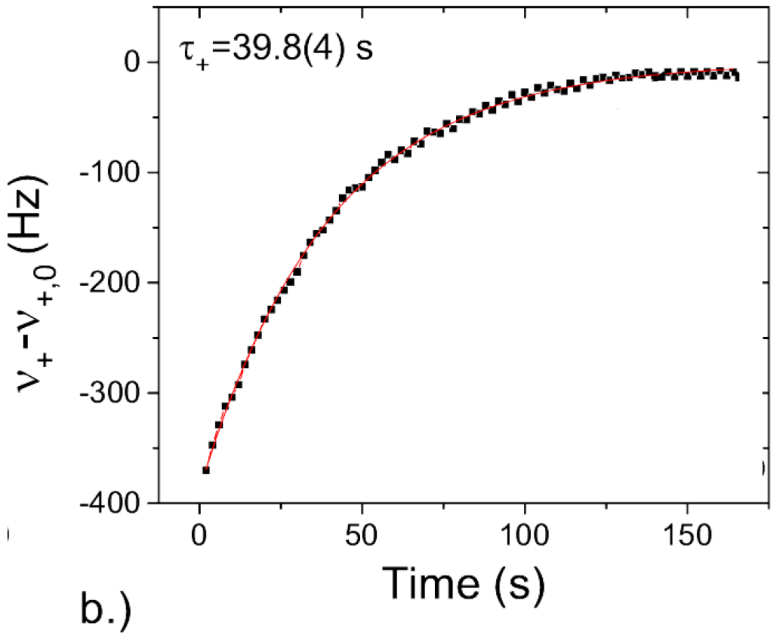

Detection in thermal equilibrium

Harmonic Oscillator:

$$\frac{F}{m} = \dot{v} + m\,\omega^2 \int v\,dt$$

Voltage in a series LC circuit:

$$V = L\frac{dI}{dt} + \frac{1}{C}\int I\,dt$$

$$I = \frac{q}{D}v$$

$$L = m\frac{D^2}{q^2}$$

$$C = \frac{1}{m\,\omega^2}\frac{q^2}{D^2}$$

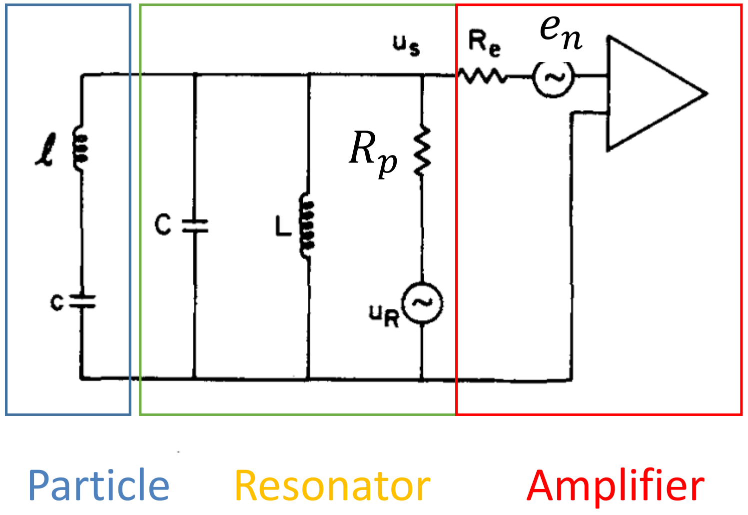

A single antiproton:

$L = 6$ MH

$C = 3 \times 10^{-21}$ F

D.J. Wineland, H.G Dehmelt, J. Appl. Phys. 46, 919 (1975)

“Particle Dip”

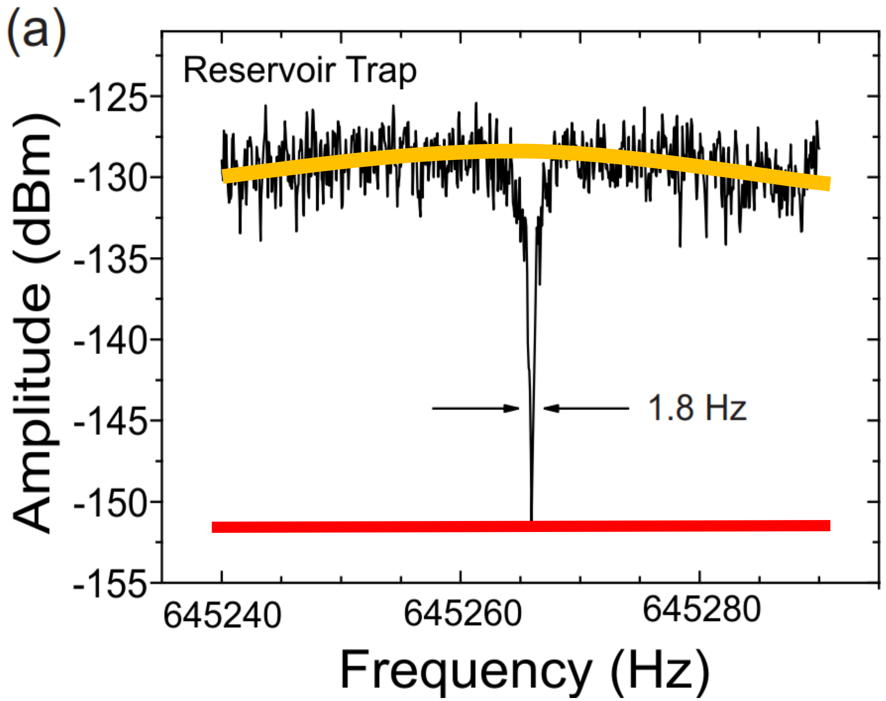

Johnson noise:

$u_n = \sqrt{4\,\pi\,k_B\,T\,Z(\omega)}$

Equivalent input noise: e_n

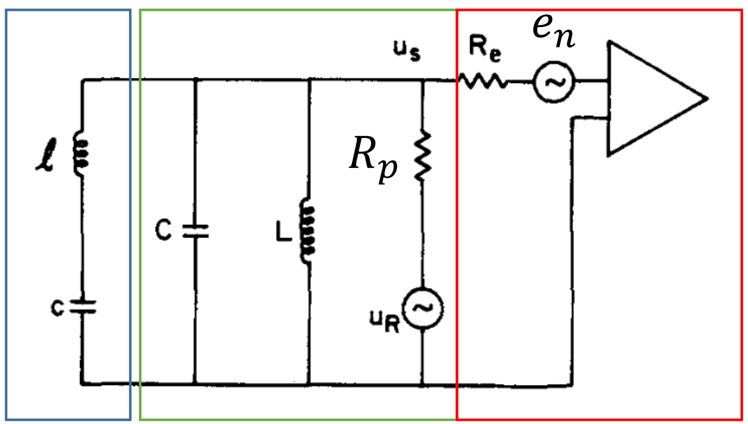

Particle Resonator Amplifier

A good dip detector has:

High parallel resistance resonator

Low equivalent input noise

$$\frac{S}{N} = \frac{\sqrt{4\,\pi\,k\,T\,R_p}}{e_n}$$

Dip properties

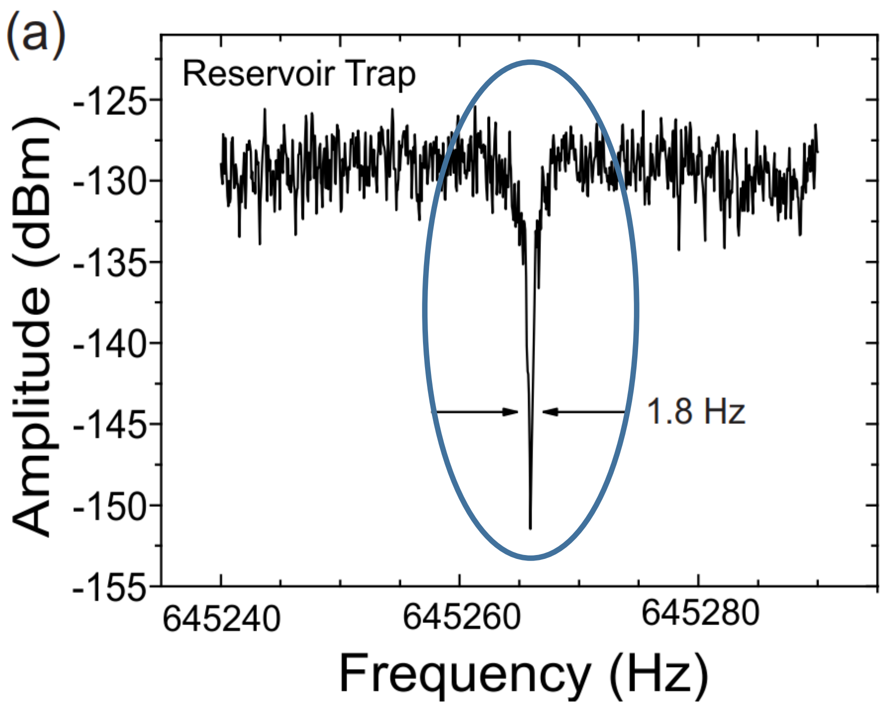

Dip line calculated from the circuit impedance:

$$\Delta\nu = \frac{1}{2\pi}\frac{q^2}{m}\frac{R_p}{D^2}$$

Axial mode:

$R_p \sim 40\ \mathrm{M\Omega}$
$\Delta\nu \sim 1\ \mathrm{Hz}$

$$R_p = \frac{Q}{2\pi\,\nu\,C}$$

Cyclotron mode:

$R_p \sim 800\ \mathrm{k\Omega}$
$\Delta\nu \sim 20\ \mathrm{mHz}$

Particle Counting

$$\Delta\nu = \frac{1}{2\pi}\frac{N\,q^2}{m}\frac{R_p}{D^2}$$

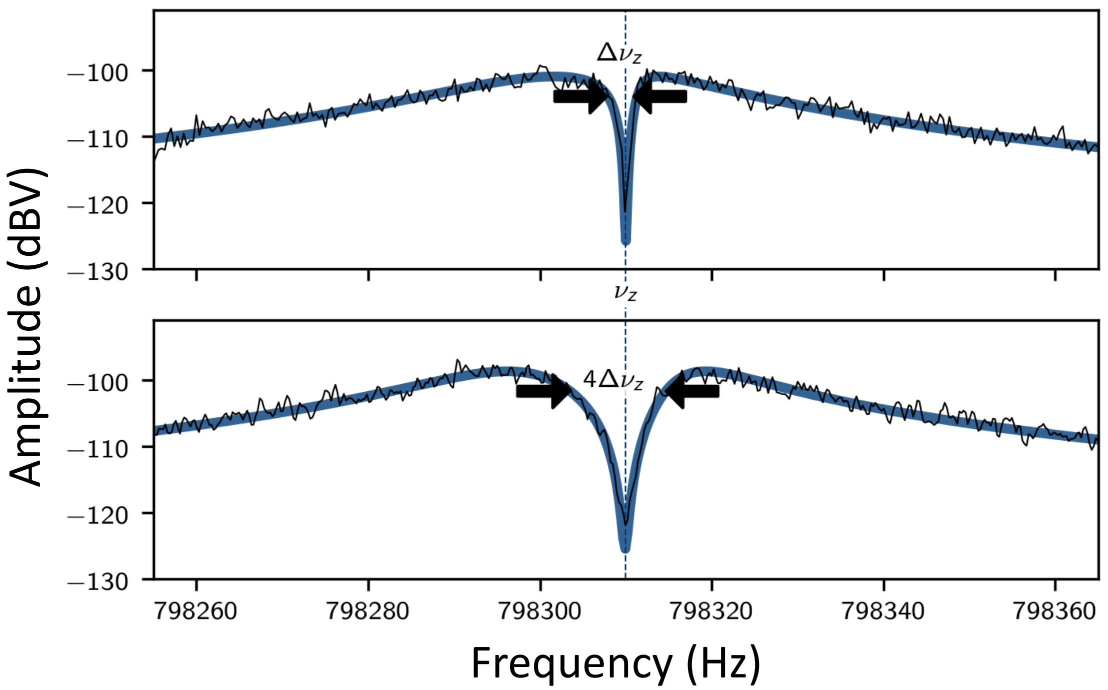

Application: Antiproton Lifetime limits

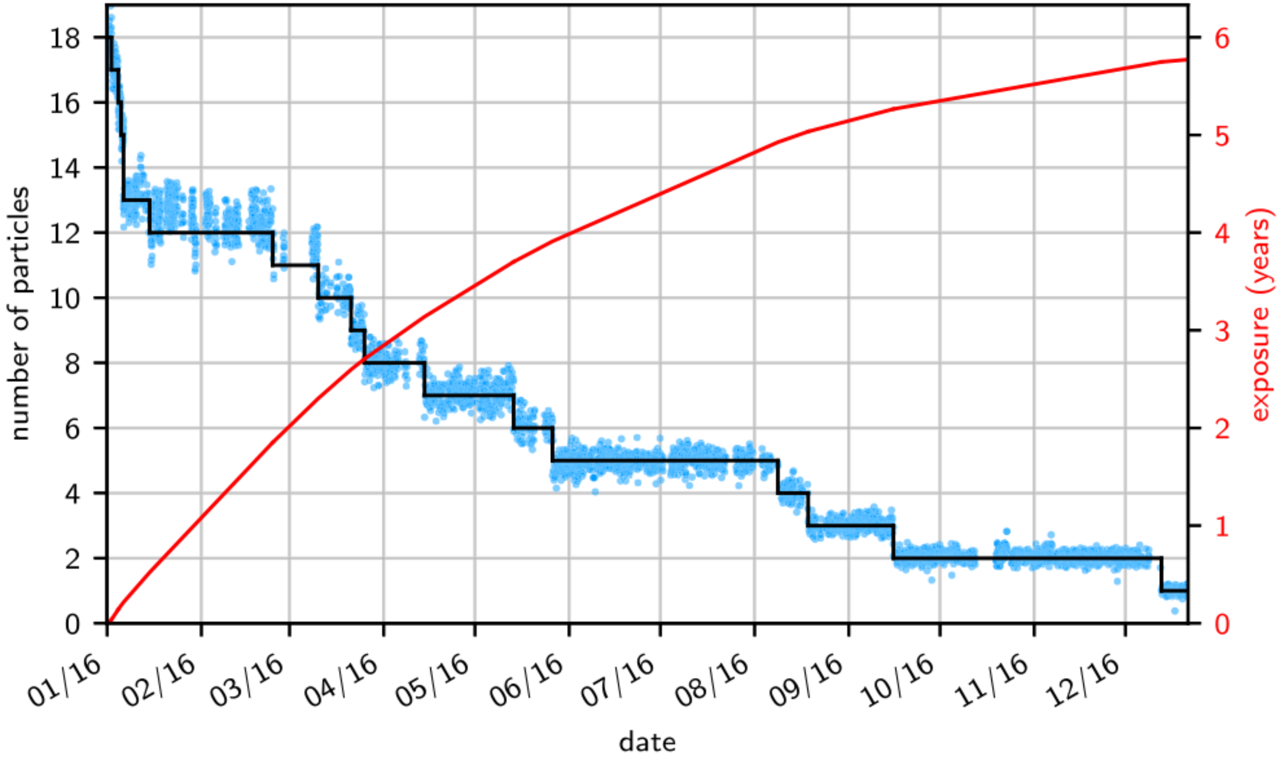

S. Sellner et al., New J. Phys. 19, 083023 (2017).

Sideband detection

Some motivation:

- Measurement of the magnetron frequency
  - Direct resistive damping leads to particle loss
  - No direct image-current detection possible

- Measurement of the modified cyclotron frequency in thermal equilibrium
  - Peak measurements require a solid energy calibration to be accurate

- Sideband cooling of the radial modes
  - Low motion amplitudes reduce systematic frequency shifts due to trap imperfections

Principle

A quadrupole rf-signal at the beat frequency couples two harmonic oscillator modes:

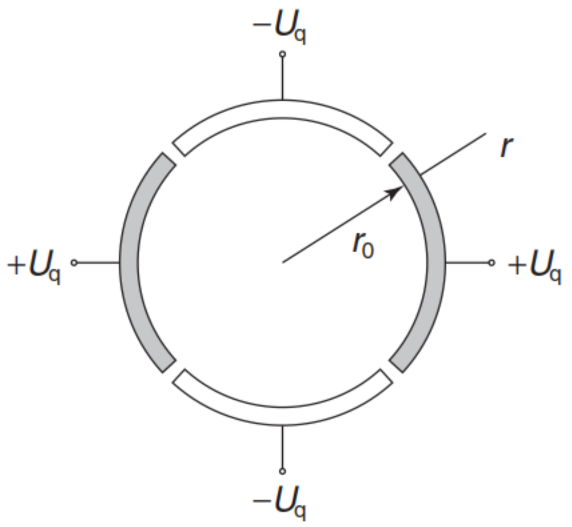

Periodic exchange of amplitudes between the modes

32 *K. Blaum*

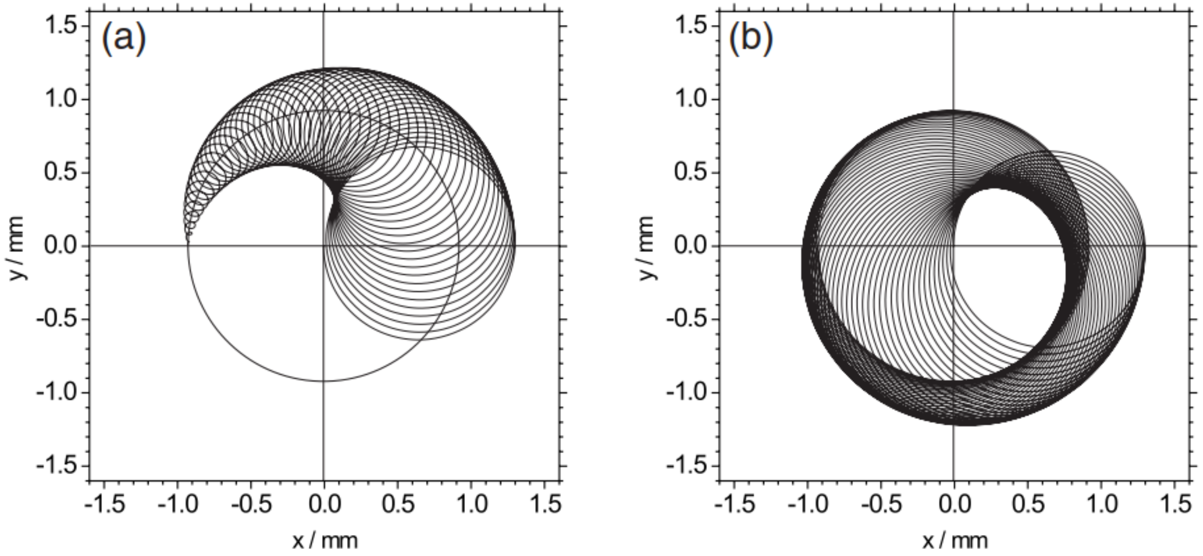

Figure 17. Conversion of a pure magnetron motion in a pure cyclotron motion in the case of azimuthal quadrupole excitation at $\nu_{rf} = \nu_c$. The motion starts with pure magnetron motion, indicated by the solid circle. Part (a) and (b) show the first and second half of the conversion.

K. Blaum, Phys. Rep. 425, 1 (2006).

Sideband FFT signal

- Averaging the FFT over several exchange cycles results in the signal of an amplitude modulated motion:

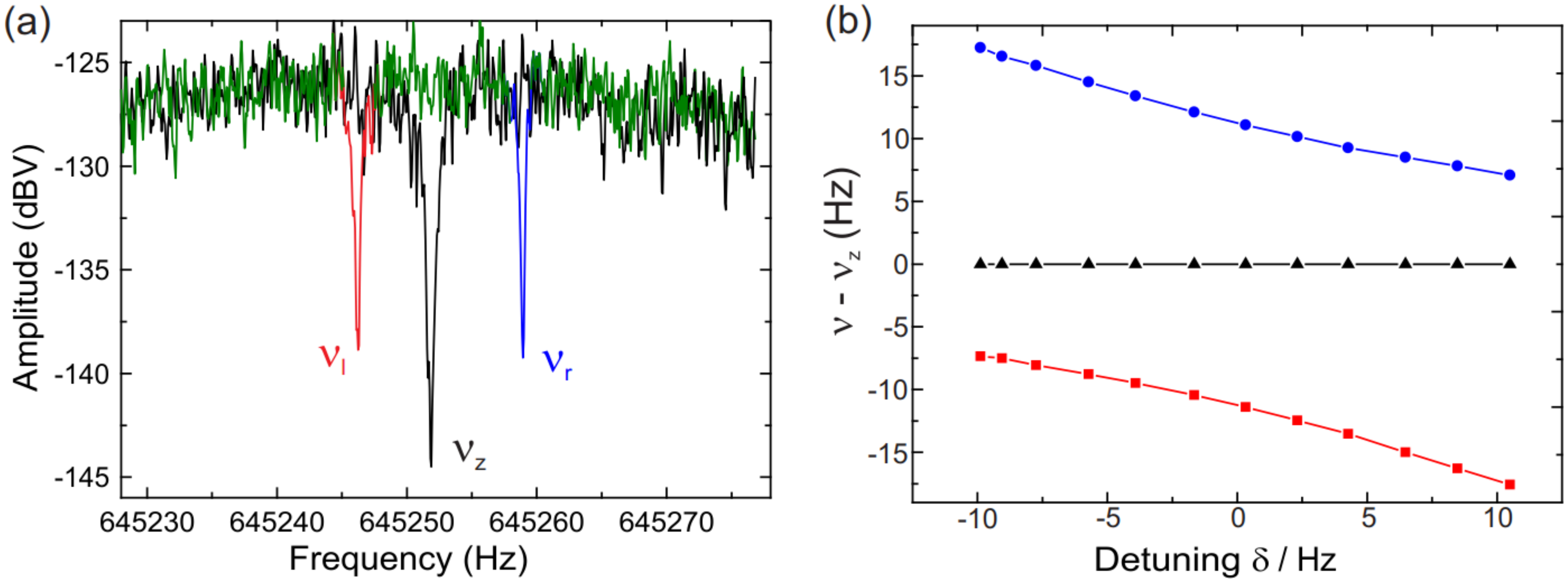

$$z(t) = z_0 \sin\left(\frac{1}{2}\Omega t\right)\cos(\omega_z t)$$

$$\nu_{l,r} = \nu_z - \frac{\delta}{2} \pm \sqrt{\frac{\Omega_0^2}{4\,\pi^2} + \delta^2}$$

Sideband measurement of the cyclotron frequency

1. Axial dip without sideband drive
2. FFT Reset
3. Double dip with slightly detuned sideband drive
4. FFT Reset
5. Double dip with adjusted sideband drive frequency
6. …

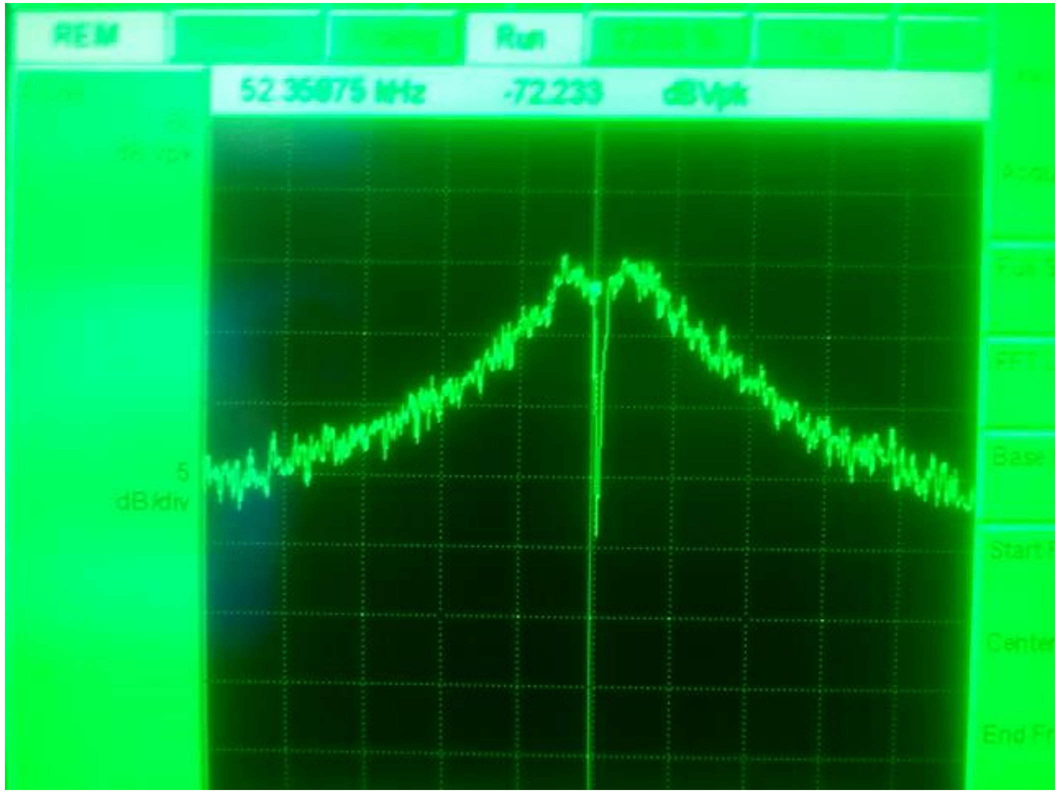

Single particle sideband coupling

- Radial frequency measurements:

$$\nu_+ = \nu_{rf} + \nu_l + \nu_r - \nu_z$$

$$\nu_c^2 = \nu_+^2 + \nu_z^2 + \nu_-^2$$

- 5.5 ppb cyclotron frequency ratio measurement in 4 mins

- 6500 frequency ratios / 35 days

  Antiproton charge-to-mass ratio with 69 ppt uncertainty

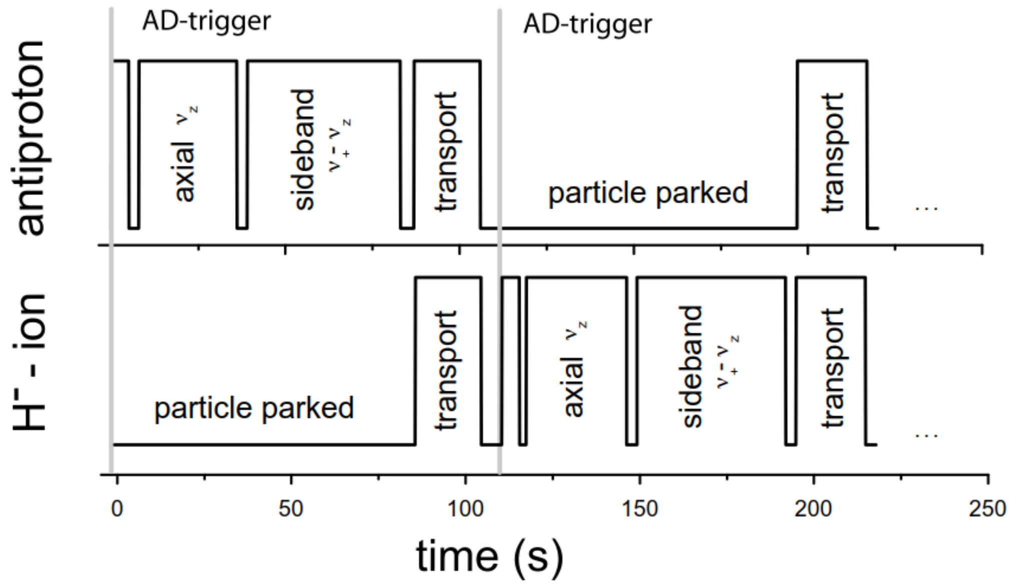

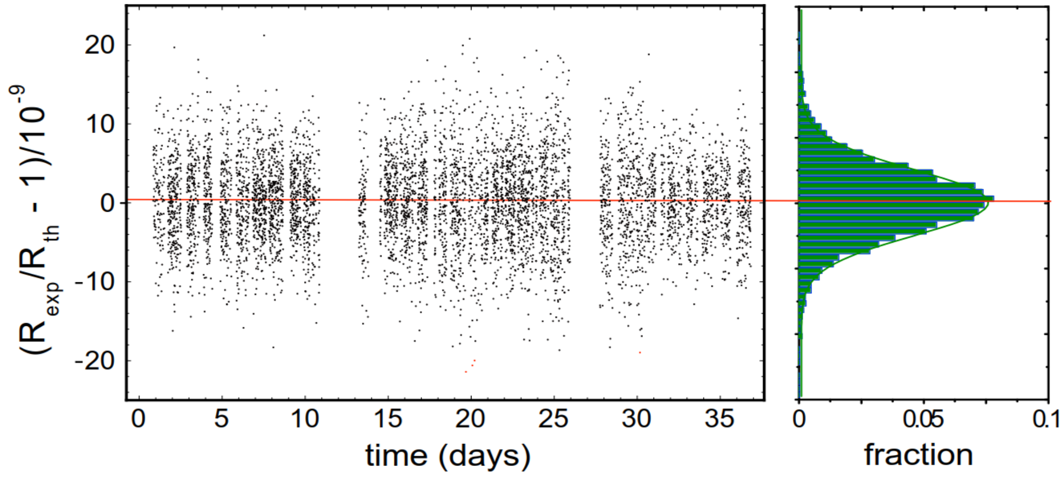

Sideband cooling limit

Cooling transition rate: Operator $a_z^* a_- \;\Longrightarrow\; \propto (k+1)\, l$

Heating transition rate: Operator $a_-^* a_z \Longrightarrow\; \propto k\,(l+1)$

Thermal equilibrium is reached when the quantum numbers are equal.

$$T_- = \frac{\nu_-}{\nu_z} T_z \sim 10 \text{ mK}$$

$$T_+ = \frac{\nu_+}{\nu_z} T_z \sim 300 \text{ K}$$

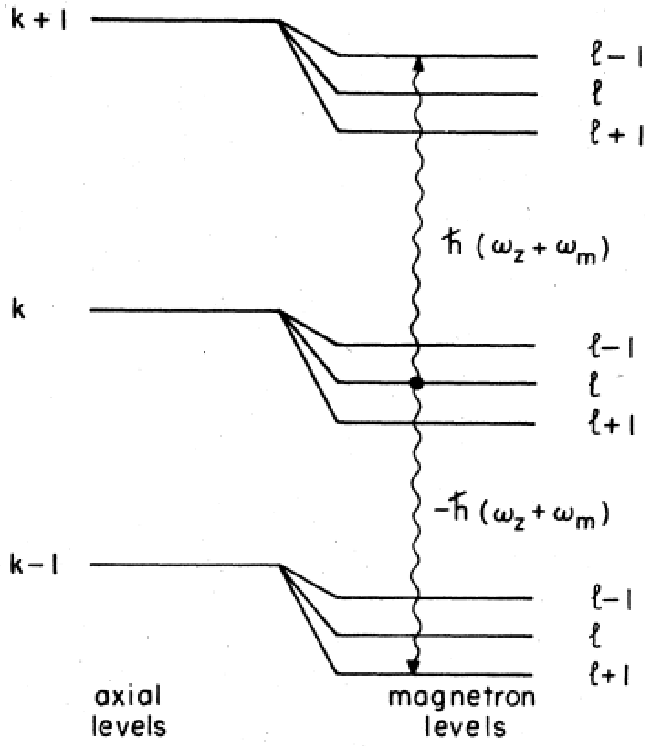

FIG. 16. Energy levels for combined axial and magnetron oscillations, with quantum numbers k and l, respectively.

L.S. Brown, G. Gabrielse, “Geonium theory” Rev. Mod. Phys. (1986).

Magnetron sideband cooling (part I)

1. Asymmetric dip due to large magnetron radius
2. Noise pulse from sideband drive generator
3. Cooling of the magnetron radius
   Frequency shift of the sideband signals
4. Double-dip signal of the magnetron-axial coupling

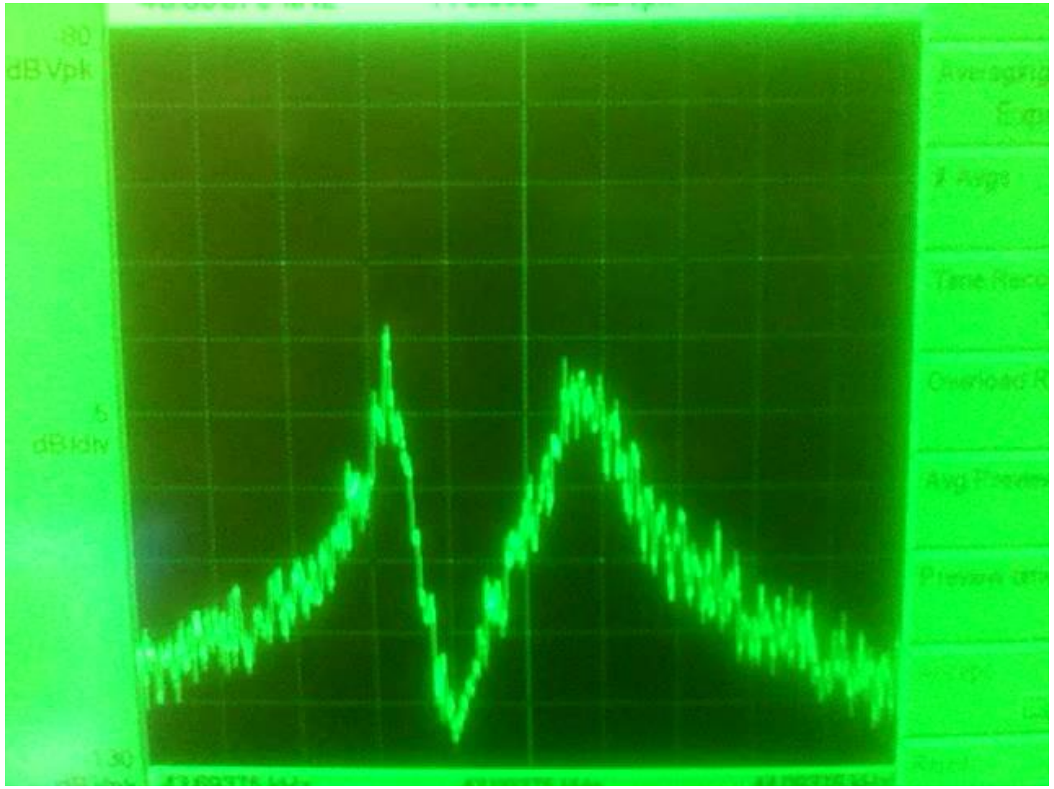

Magnetron sideband cooling (part II)

1. Noise pulse from switching of the sideband drive generator
2. Axial frequency at the sideband cooling limit
3. Cooling of the axial mode
   S/N increases over the time span of several minutes

Construction of image current detectors

Axial Frequency (700 kHz) Detection Systems

Low resistance inductor of the axial frequency

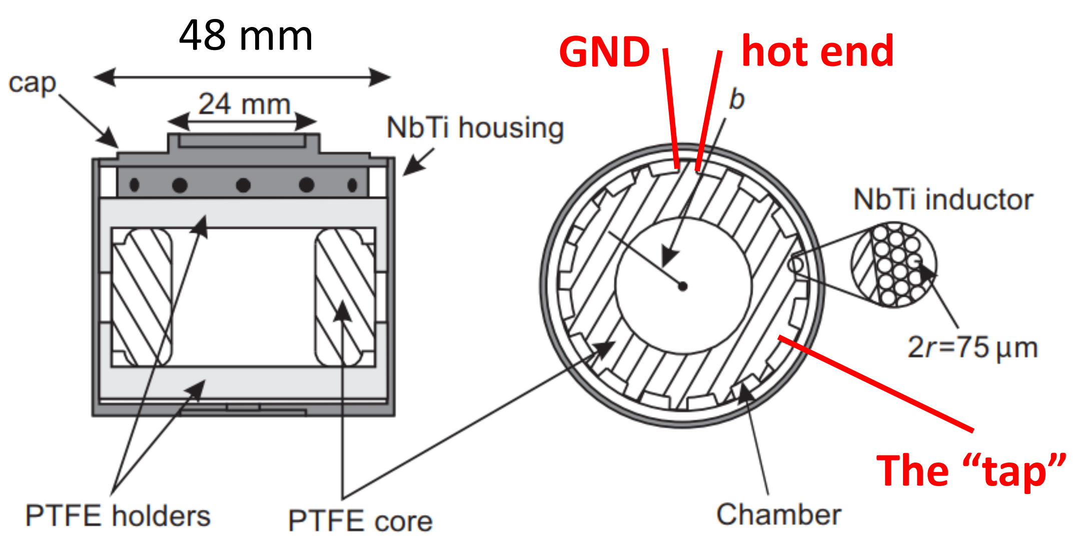

- PTFE insulated superconducting NbTi wire
- A PTFE support core / housing
- Thread seal tape (Teflon)
- Superconducting rf-Resonator
- Annealed copper wire
- Some soldering equipment

Resonator

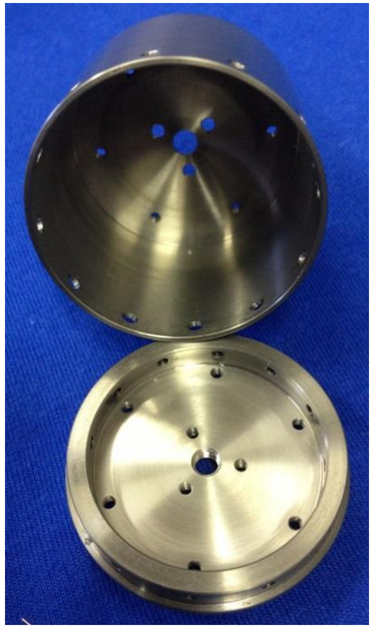

Toroidal coil

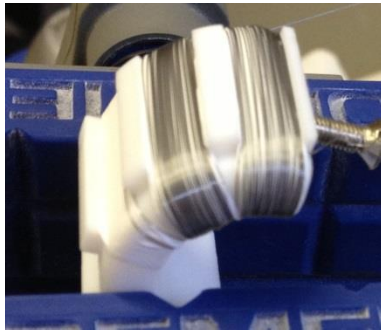

N = 950 – 1200
Q = 200k – 500k
L = 2-3 mH
Rp > 1 GΩ

Essential:

- Superconductors are very poor heat conductors! Radiation shielding is very important!
- Good soldering joints!

H. Nagahama *et al.*, Rev. Sci. Instr. **87**, 113305 (2016).

Some installation details

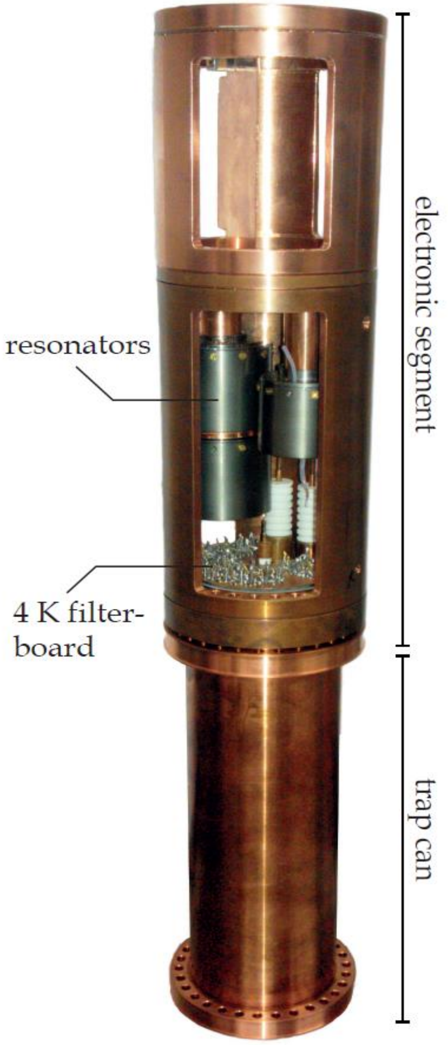

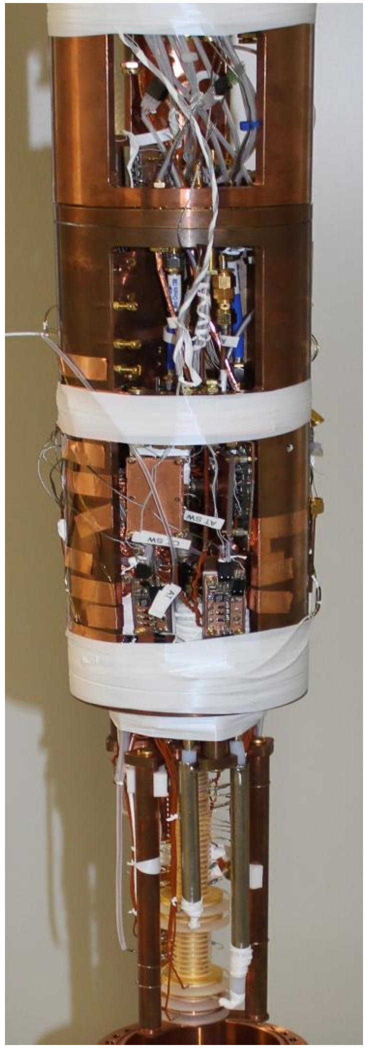

+ 0.5 mm PTFE shield
+ 20 layers of MLI foil

Annealed copper wire
Sapphire feedthroughs

No radiation windows

6 K temperature

1.9 T magnetic field

Cyclotron detection system @ 30 MHz

Copper resonator

Teflon bobbin

NbTi coil

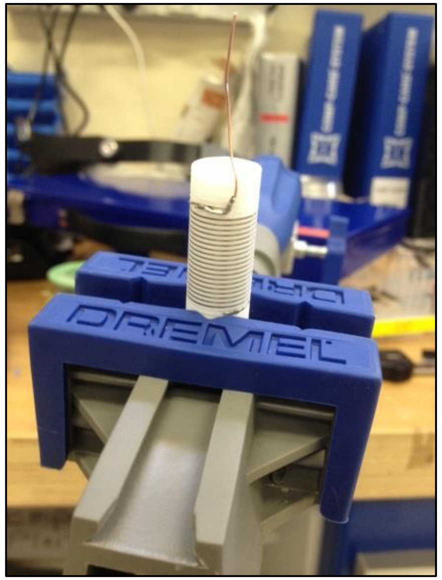

4K amplifier

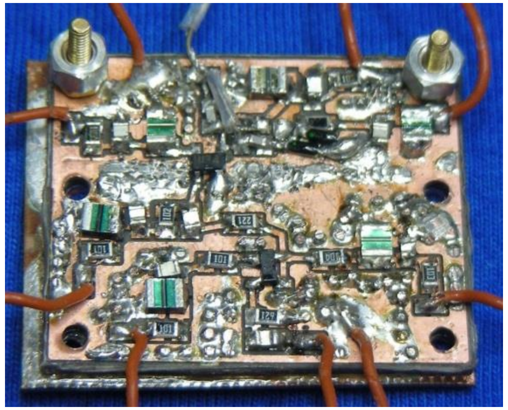

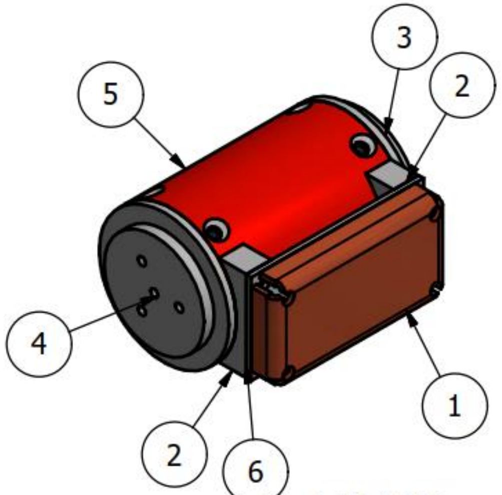

VIEW2
SCALE 1 : 1

Dimensions:
Diameter: 26 mm
Length: 41.5 mm

Inductance: 1 uT
Parasitic Capacitance: 24 pF
Resonance frequency: 30 MHz

Realistic Cyclotron Detection Circuit

Apply DC voltage both parts of the segmented electrode

Resonance frequency matching to the cyclotron frequency

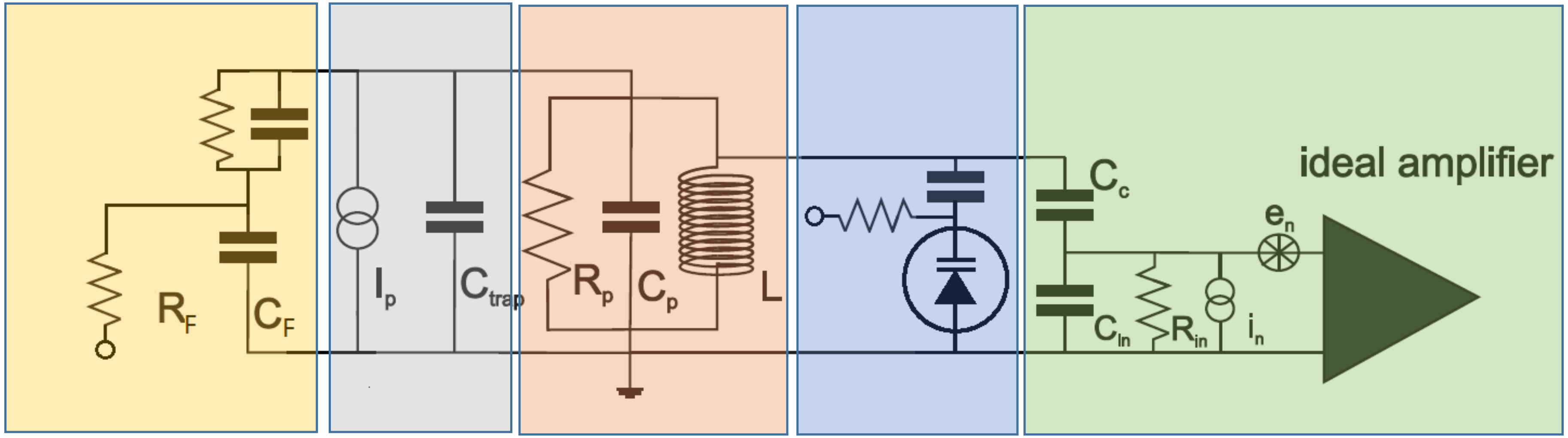

Trap biasing | Trap | Resonator | Varactor | Amplifier

Amplifier with parasistic properties:

- Voltage noise and current noise (< 1 nV)
- Miller-feedback
- Input resistance (large, > 100 kOHm @ 30 MHz)
- Input capacitance (small, typically 2 pF)

S. Ulmer *et al.*, Nucl. Instr. Meth. A **705**, 55-60 (2013).

Amplifier Layout

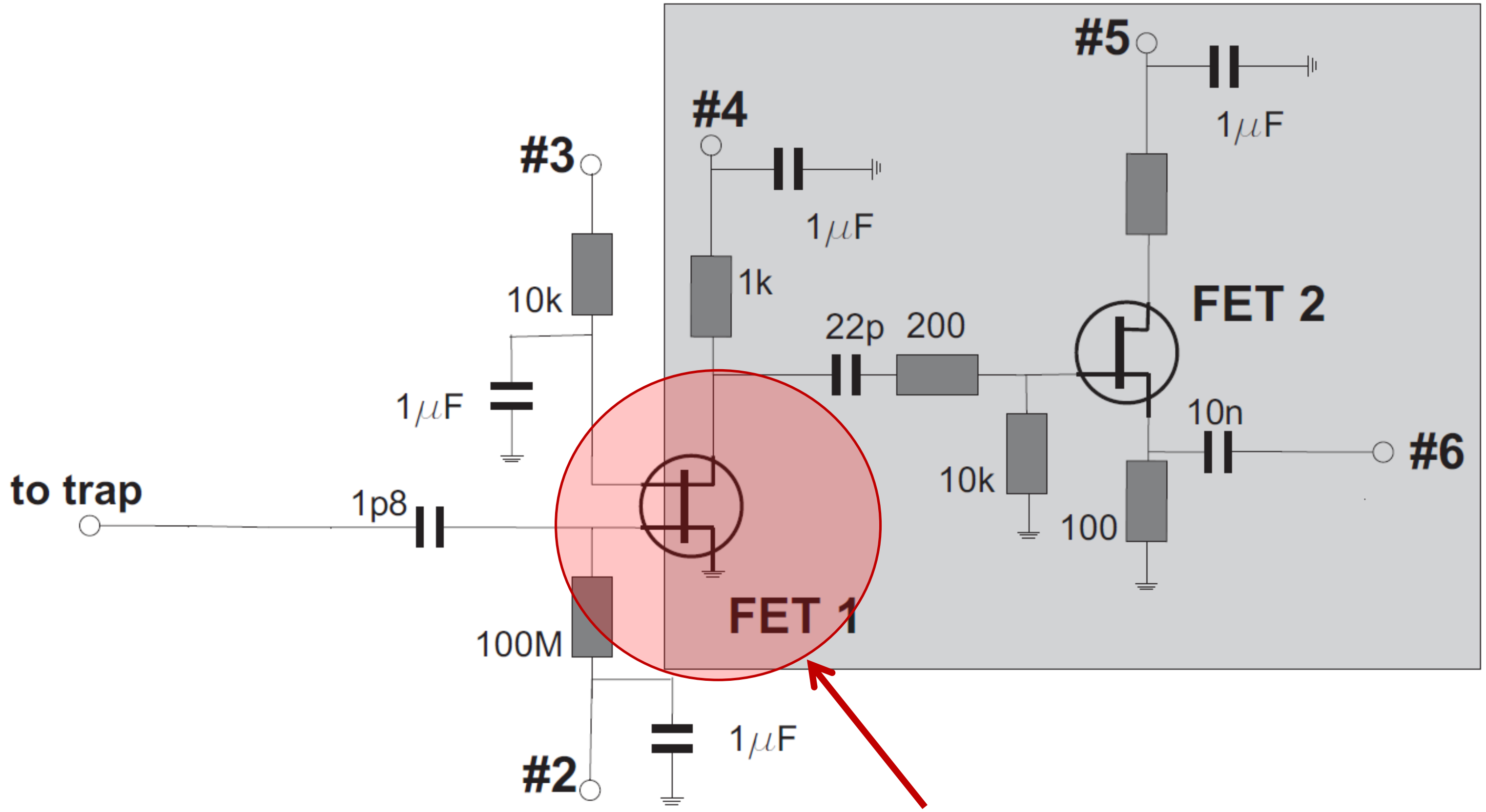

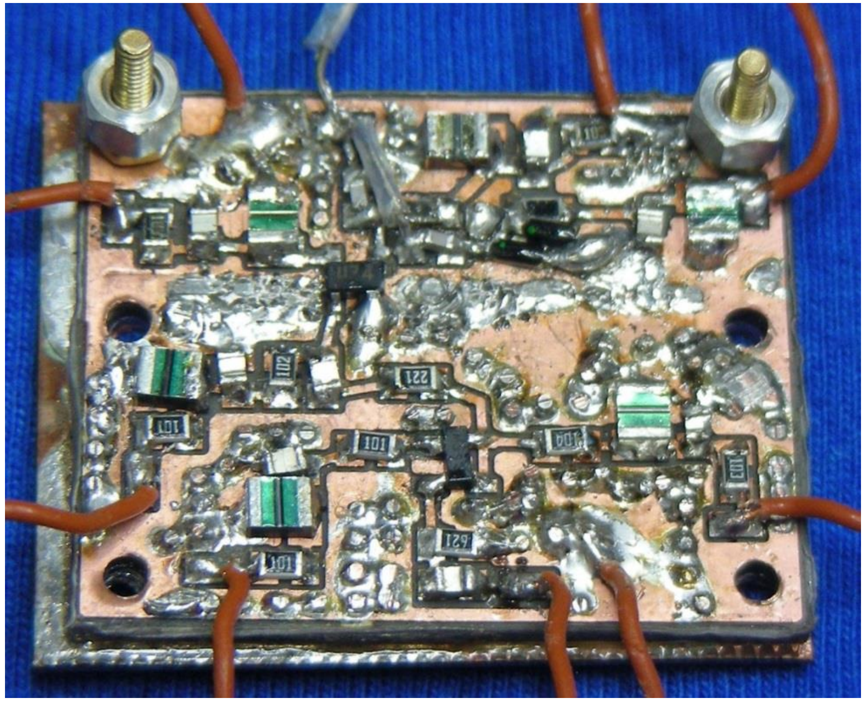

GaAs dual gate FETs: examples: 3SK166, CF739, NE25139, 3SK177

FET 1:
Decoupling of the resonator and the readout
Amplification
FET 2:
Source follower – 50 Ohm impedance matching

Cyclotron Detector Q-Value as function of the gate voltage

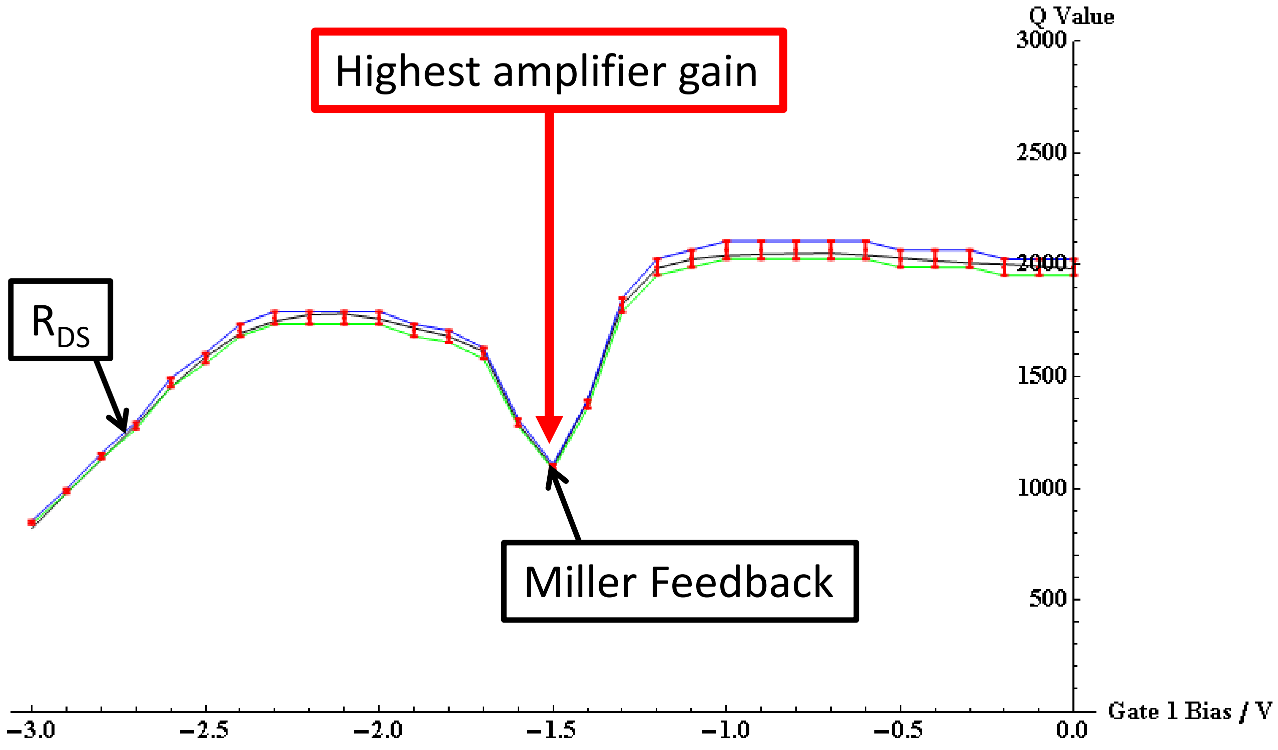

Limitations of the Cyclotron Detector

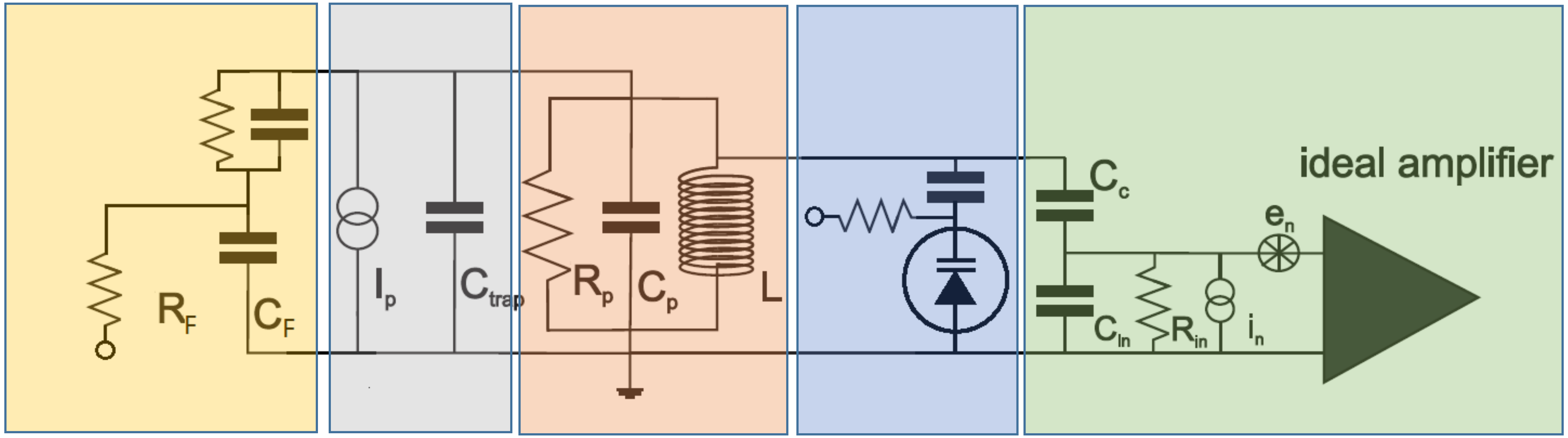

Trap biasing | Trap | Resonator | Varactor | Amplifier

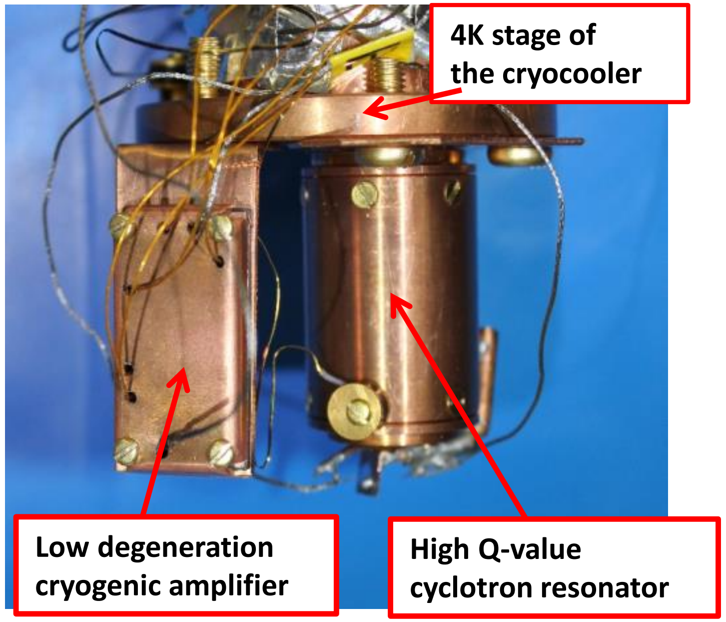

Component	R_p
Resonator @ 30 MHz	1.4 MΩ
Trap Biasing Network	2.7 MΩ
Varactors	> 10 MΩ
Amplifier (κ^2 @ 1/25)	4.8 MΩ
Total System	740 kΩ

S. Ulmer *et al.*, Nucl. Instr. Meth. A **705**, 55-60 (2013).

Other antiproton detection methods

- Self-excited antiproton oscillator (Image-current technique)
- Stochastic cooling / Schottky pickup (Image-current technique)
- Destructive detection methods
  - Annihilation products using scintillation detectors
  - Charge-amplifiers / secondary electron multipliers
- Under development:
  Optical detection via a controlled coupling of beryllium ions to (anti)protons
  BASE Hannover (C. Ospelkaus et al.), BASE-Mainz (M. Bohman, M. Wiesinger et al.

…

Thank you for your attention!


H. Nagahma
RIKEN / Tokyo


J. A. Devlin
RIKEN


S. Ulmer
RIKEN


A. Mooser
RIKEN


M. Wiesinger
U - Mainz


C. Smorra
CERN / RIKEN


E. Wursten
MPI-K / CERN


M. Bohman
MPI-K / RIKEN

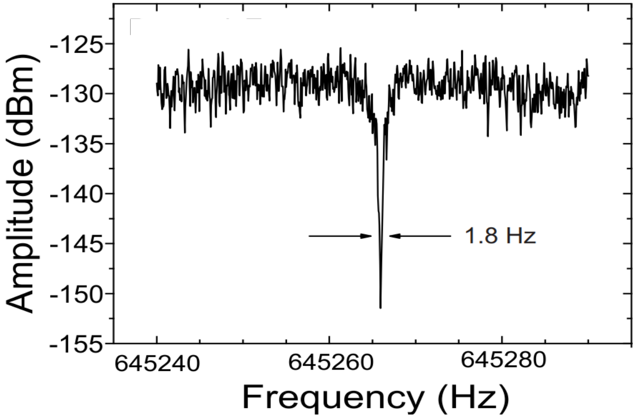


S. Sellner
RIKEN

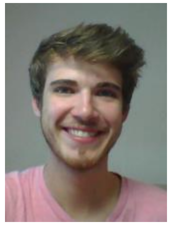
Pascal E. Blessing
GSI


T. Higuchi
RIKEN / Tokyo

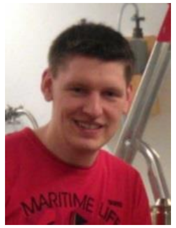
G. Schneider
U - Mainz

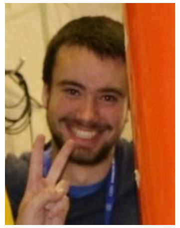
M. Borchert
U - Hannover


J. Harrington
RIKEN & MPIK